Journal of Physics D: Applied Physics

PAPER

Experimental analysis of the Schottky barrier height of metal contacts in black phosphorus field-effect transistors

To cite this article: Hsun-Ming Chang *et al* 2018 *J. Phys. D: Appl. Phys.* **51** 135306

View the article online for updates and enhancements.

This content was downloaded from IP address 140.112.4.67 on 09/03/2018 at 16:33

J. Phys. D: Appl. Phys. **51** (2018) 135306 (8pp) https://doi.org/10.1088/1361-6463/aab063

Experimental analysis of the Schottky barrier height of metal contacts in black phosphorus field-effect transistors

Hsun-Ming Chang[1], Kai-Lin Fan[2], Adam Charnas[5], Peide D Ye[5], Yu-Ming Lin[3], Chih-I Wu[1,4] and Chao-Hsin Wu[1,2]

[1] Graduate Institute of Photonics and Optoelectronics, National Taiwan University, No. 1, Sec. 4, Roosevelt Road, Taipei 10617, Taiwan (R.O.C)
[2] Graduate Institute of Electronics Engineering, National Taiwan University, No. 1, Sec. 4, Roosevelt Road, Taipei 10617, Taiwan (R.O.C)
[3] Taiwan Semiconductor Manufacturing Company, No. 8, Li-Hsin Rd. 6, Hsinchu Science Park, Hsinchu City 300, Taiwan (R.O.C)
[4] Industrial Technology Research Institute. 195, Sec. 4, Chung Hsing Rd., Chutung, Hsinchu City 31040, Taiwan (R.O.C)
[5] School of Electrical and Computer Engineering and Birck Nanotechnology Center, Purdue University, West Lafayette, IN 47907, United States of America

E-mail: ymlinw@tsmc.com (Y-M Lin) and chaohsinwu@ntu.edu.tw (C-H Wu)

Received 4 December 2017, revised 15 February 2018
Accepted for publication 19 February 2018
Published 8 March 2018

Abstract

Compared to graphene and MoS_2, studies on metal contacts to black phosphorus (BP) transistors are still immature. In this work, we present the experimental analysis of titanium contacts on BP based upon the theory of thermionic emssion. The Schottky barrier height (SBH) is extracted by thermionic emission methods to analyze the properties of Ti-BP contact. To examine the results, the band gap of BP is extracted followed by theoretical band alignment by Schottky–Mott rule. However, an underestimated SBH is found due to the hysteresis in electrical results. Hence, a modified SBH extraction for contact resistance that avoids the effects of hysteresis is proposed and demonstrated, showing a more accurate SBH that agrees well with theoretical value and results of transmission electron microscopy and energy-dispersive x-ray spectroscopy.

Keywords: black phosphorus, contact resistance, Schottky barrier height, MOSFET, metal contact

(Some figures may appear in colour only in the online journal)

Two-dimensional (2D) materials have shown some great material properties in next-generation electronic applications such as a naturally thin body, atomically smooth interface, high carrier mobility and tunable band gap. Amongst all 2D materials, graphene is firstly discovered [1]. While graphene shows a high carrier mobility that exceeds 100 000 cm^2 V^{-1} s^{-1} and good thermal conductivity, the absence of band gap energy leads to poor current on/off ratio, thus restraining its further application to electronics [2]. On the other hand, transition metal dichalcogenides (TMDs) such as MoS_2 and WSe_2 demonstrate a larger band gap that provides a large I_{ON}/I_{OFF} of above 10^8; however, the relatively low carrier mobility at the order of 10–10^2 cm^2 V^{-1} s^{-1} constrains the high speed application [3–5]. Black phosphorus (BP) has been recently rediscovered to be an attractive 2D semiconductor for high-performance transistor devices [6, 7]. Like other 2D materials, BP is composed of covalent bonding of P atoms inside each layer and the stacking of each layer by van der Waals (vdW) interactions. BP is a naturally p-type semiconductor revealing a tunable direct band gap ranging from 0.3 eV for bulk to 1.5–2 eV for monolayer [8, 9]. Moreover, a high carrier mobility exceeding 1000 cm^2 V^{-1} s^{-1} can be obtained at room temperature [8, 10]. The above

 © 2018 IOP Publishing Ltd Printed in the UK

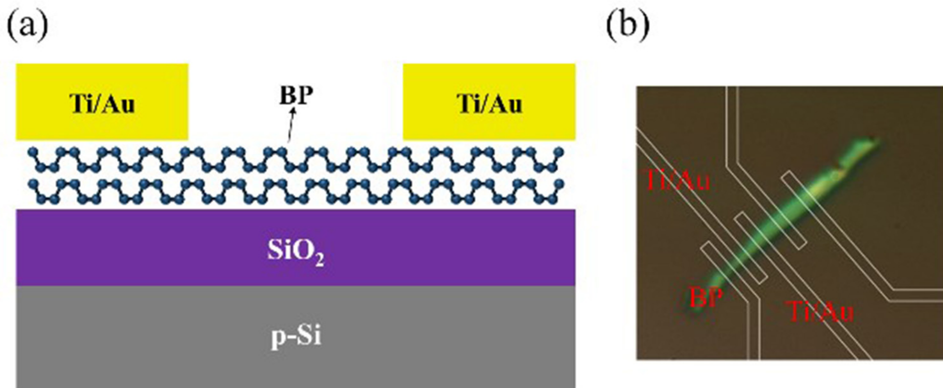

Figure 1. (a) Schematic structure of the back gate BP FET. (b) Optical microscopy picture of the Ti-contact BP transistor.

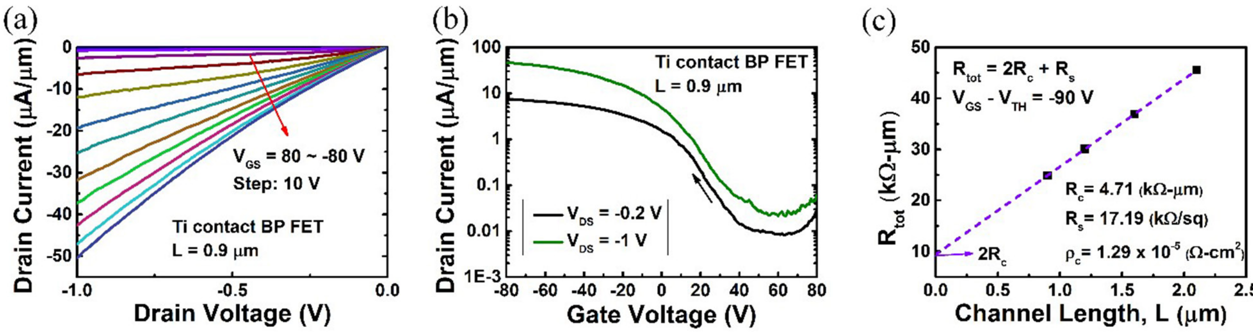

Figure 2. (a) Output characteristics. (b) Transfer curve where the arrow represent the sweeping direction of gate bias. (c) TLM results of a Ti contact BP transistor.

advantages of BP bridge the gap between graphene and TMDs, making BP a promising layered material for high-performance electronics as well as optoelectronics applications [11]. However, comprehensive understanding of BP-metal contacts, which is a crucial issue in 2D materials, is still lacking. For a typical back-gate BP transistor without any treatment in contact regime, the transport characteristics are highly influenced by the metal/BP contact, which can be described by Schottky barrier (SB) MOSFET model [12]. For a high work function metal such as palladium (Pd), more hole carriers are injected into the contact due to the lower Schottky barrier height (SBH), hence improving the p-type performance [13, 14]. On the contrary, a low work function metal such as aluminum (Al) contributes to n-type performance due to the lower SBH for electron carriers [15, 16]. Hence, to enhance the electrical performance of BP transistors, it is important to understand the magnitude of SBH.

In this work, we fabricate back-gate BP transistors with titanium (Ti) as metal contacts and extract SBH of BP-metal contact by low temperature electrical measurements. Compared with a theroretical SBH based on bandgap alignment, we found that extracted SBH can be underestimated due to the hysteresis on BP channel. A modified SBH extraction for contact resistance that avoids the effects of hysteresis is thus developed, which results in a more accurate SBH value in accordance with theoretical prediction.

Results and discussion

Few-layer BP flakes used in this study were mechanically exfoliated from bulk crystal and then transferred onto p-doped silicon substrates covered with 260 nm SiO_2. The exfoliation and transfer processes were performed inside a glove box filled with nitrogen to reduce moisture absorption and oxidation of BP. After exfoliation, the sample was cleaned by acetone and source/drain (S/D) contact were defined through standard electron beam lithography (EBL) process, followed by 10/60 nm Ti/Au metal deposition to complete a back-gate BP transistor. The schematic device structure is shown in figure 1(a), where the thickness is about 10–11 nm estimated from the contrast under optical microscope, as shown in figure 1(b). After device fabrication, the device was loaded into a vacuum chamber immediately for electrical measurement.

The output characteristics and transfer curve of a BP FET with channel length (L) of 0.9 μm are shown in figures 2(a) and (b), respectively. The output characteristics show a slightly non-linear I_D–V_D behavior at small V_{DS}, indicating a Schottky contact. The extracted R_{ON} is 77.48 k$\Omega \cdot \mu$m at a gate overdrive of −40 V. As shown in figure 2(b), the I_{ON}/I_{OFF} ratio is 10^3 and the extrinsic hole mobility is 55.6 cm^2 V^{-1} s^{-1} extracted by $\mu_{eff} = G_m L/(C_{ox} W V_{DS})$, where C_{ox}, W, L, and G_m are oxide capacitance, channel width, channel length, and the peak transconductance, respectively. In addition, a device with a transfer length method (TLM) structure is fabricated for contact resistance (R_c) extraction. The contact resistance is extracted as 4.71 k$\Omega \cdot \mu$m at a gate overdrive of −90 V, as shown in figure 2(c).

SBH can be derived using commonly-used method for 2D materials, where SBH is extracted through the activation energy in the thermionic emission regime [17, 18]. There are two mechanisms for carrier injection from metal to

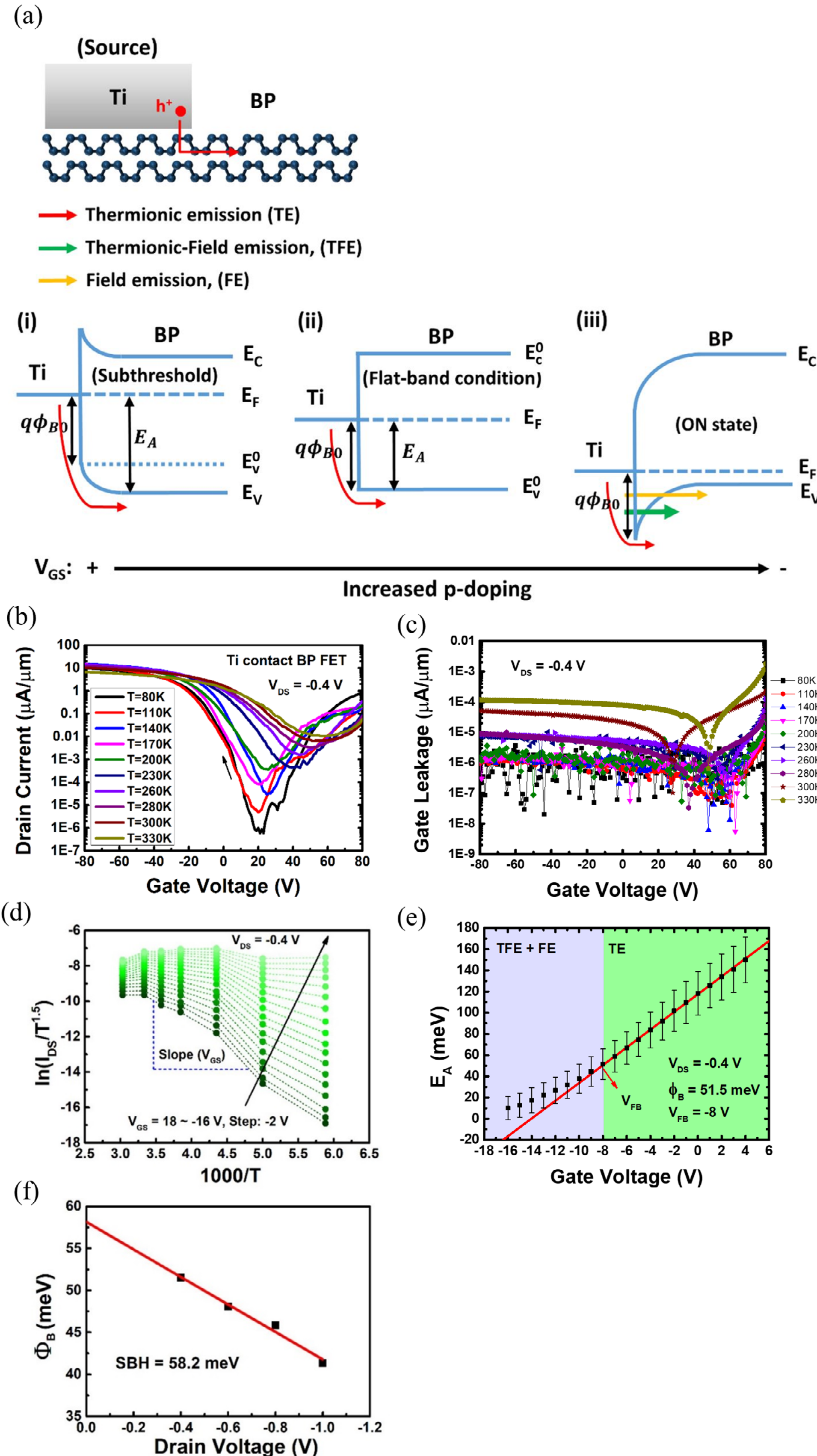

Figure 3. (a) Typical conditions of M-S junction band alignment and carrier injection mechanism at different V_{GS}. (b) I_{DS}–V_{GS} at various temperature where V_{GS} sweeps from positive to negative. Characteristics of thermionic emission are observed at subthreshold region. (c) Gate leakage current versus V_{GS} at various temperatures. (d) Arrhenius plot of various V_{GS} in subthreshold regime. (e) Activation energy (E_A) versus V_{GS} with error bars, where the SBH can be obtained at flat-band condition V_{FB}. (f) Extracted SBH versus V_{DS}, where the SBH without barrier lowering induced by image force can be obtained.

semiconductor: thermionic emission (TE) and field emission (FE). To simplify the analysis without loss of generality, the voltage drop at drain is considered negligible due to the large forward bias carrier injection at large enough V_{DS}. Hence, electrical transport from metal to a 2D material in source contact can be described by reverse bias TE equation [18]:

$$I_{DS} = AA^*T^{1.5}e^{-\frac{q\phi_B}{kT}}\left(1 - e^{-\frac{qV}{kT}}\right) \quad (1)$$

where A is the contact area, A^* is the Richardson constant, ϕ_B is the effective Schottky barrier height, k is the Boltzmann constant and V is the voltage drop at source contact. When $V \gg \frac{kT}{q}$, equation (1) can be simplified as $I_{DS} = AA^*T^{1.5}e^{-\frac{q\phi_B}{kT}}$. Typical band alignments and carrier injection mechanisms of M-S junction at different V_{GS} are demonstrated in figure 3(a). E_c^0 and E_v^0 are conduction band and valence band at falt band condition, respectively. In the subthreshold regime (i), the barrier height for hole is the activation energy E_A, where $E_A = q\phi_{B0} + E_V - E_v^0$. Equation (1) can thus be modified as $I_{DS} = AA^*T^{1.5}e^{-\frac{E_A}{kT}}$. When V_{GS} sweeps negatively to the flat-band condition (ii), E_A equals to the Schottky barrier height, $q\phi_{B0}$. For both (i) and (ii), the carriers are injected only by TE. Therefore, we can extract E_A from the slope of the Arrhenius plot $\ln(I_{DS}/T^{1.5})$ versus $1000/T$. However, as V_{GS} sweeps further negatively to 'ON' state (iii), the carriers are injected by not only TE but also thermionic field emission (TFE) and field emission (FE). Consequently, effective SBH extracted from the TE equation will be underestimated due to the additional carrier injection by TFE and FE. Through the relationship between E_A and V_{GS}: $E_A = q\phi_{B0} - \left(1 + \frac{C_{it}}{C_{ox}}\right)^{-1}(V_{GS} - V_{FB})$ where C_{it} and C_{ox} is the capacitance of interfacial trap and oxide, respectively, it is clear that E_A varies linearly with V_{GS} until the flat-band voltage, V_{FB}. Hence, once E_A started varies non-linearly with V_{GS}, the turnig point is the flat-band condition where E_A equals to $q\phi_{B0}$. On the other hand, to correct image force lowering effects due to the applied voltages, SBHs extracted from various V_{DS} are linearly extrapolated to zero bias. Thus, temperature-dependent I_{DS} versus V_{GS} at a fixed V_{DS} of -0.4 V is first measured. As shown in figure 3(b), I_{ON}/I_{OFF} ratio decreases and V_{TH} shifts right with increasing temperature as expected. In addition, at more negative gate bias (i.e. at 'ON' state), I_{DS} depends weakly on temperature, indicating the domination of field emission. On the other hand, at the subthreshold regime where the gate bias is less negative, I_{DS} increases as temperature increases, indicating the domination of thermionic emission. This observation is in accordance with the above derivation and SB-MOSFET model [12]. The ambipolar characteristics can also be observed in figure 3(b), which can be attributed to the low band gap of phosphorene. When the reverse bias ($V_{GS} = +40$–$+80$ V) is applied, conduction band will be close to Fermi Level, and the electron concentration will overwhelm hole concentration and becomes the dominant carrier [6]. Note that the I_{DS}–V_{GS} curve is measured in the sweeping direction of gate bias from positive to negative. Hence, the Arrhenius plot of various V_{GS} in the subthreshold regime is plotted to extract the barrier height.

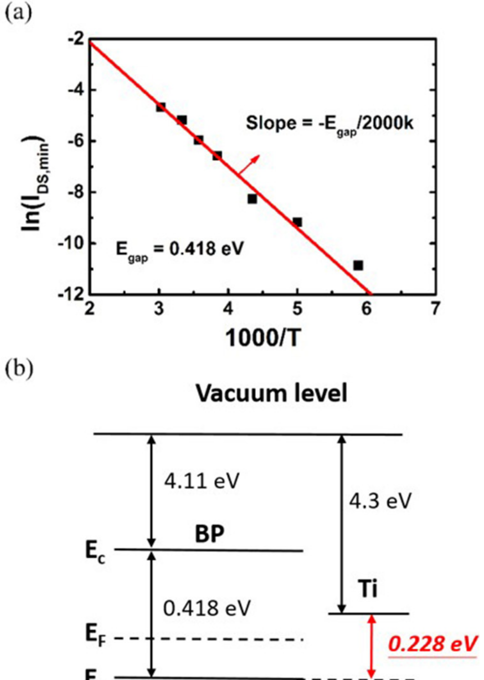

Figure 4. (a) Band gap energy Egap extracted from the relationship between minimum I_{DS} and temperature. (b) Theoretical band alignment of BP and Ti, where BP and Ti are separated without contact. The SBH is expected to be 0.228 eV.

As shown in figure 3(d), different slopes represent the activation energy E_A for each V_{GS}, which results from the band bending by gate bias. The activation energy extracted from the slope of the Arrhenius plot is plotted versus gate voltage, as shown in figure 3(e). Taking advantage of the linear relationship between E_A and V_{GS} until flat-band condition, the SBH at $V_{DS} = -0.4$ Vcan be extracted from the slope to be 51.5 meV. To account for the barrier lowering due to image charges, the SBH is thus extracted at different V_{DS} by the same method and linearly extrapolated to zero bias as shown in figure 3(f). Finally, a SBH of 58.2 meV is obtained for Ti-BP contact.

The extracted SBH is compared with the value predicted by theoretical calculation of Schottky–Mott rule. The Schottky barrier height ϕ_{B0} for hole carrier is equal to $(q\chi + E_{gap} - q\phi_M)$, where $q\chi$ is the electron affinity of semiconductor, E_{gap} is the band gap of semiconductor, and $q\phi_M$ is the metal work function. The work function of Ti is 4.3 eV, and $q\chi$ is estimated to be -4.11 eV for the few-layer BP (~10–11 nm) [19]. In the ambipolar FET, the relationship between the minimum current $I_{DS,\ min}$ and band gap energy can be described by the formula:

$$I_{DS,\ min} \propto e^{-\frac{E_{gap}}{2kT}}. \quad (2)$$

Hence, E_{gap} can be extracted through the slope of $\ln(I_{DS,\ min})$ versus $1/T$. Equation (2) can be understood by the equality of hole and electron carriers at minimum current point, which therefore is related to the relationship between intrinsic conductivity and band gap energy. As shown in figure 4(a), E_{gap} is extracted to be 0.418 eV. Compared to the theoretical calculation where $E_{gap} = 0.39\,\text{eV} + 1.62/n^{1.4}$ (n = number of

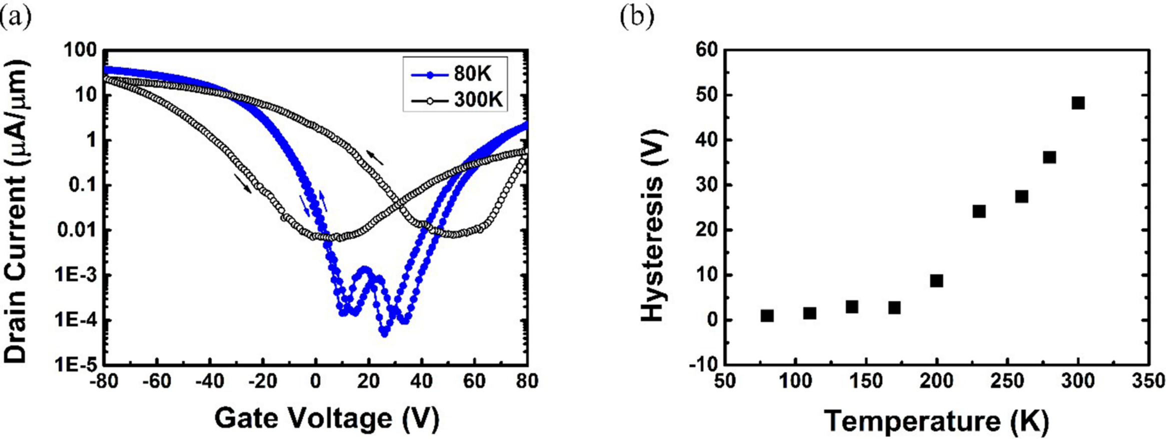

Figure 5. (a) Hysteresis observed in I_{DS}–V_{GS} at 80 K and 300 K. (b) Hysteresis versus temperature, where hysteresis become obvious as T increases over 170 K.

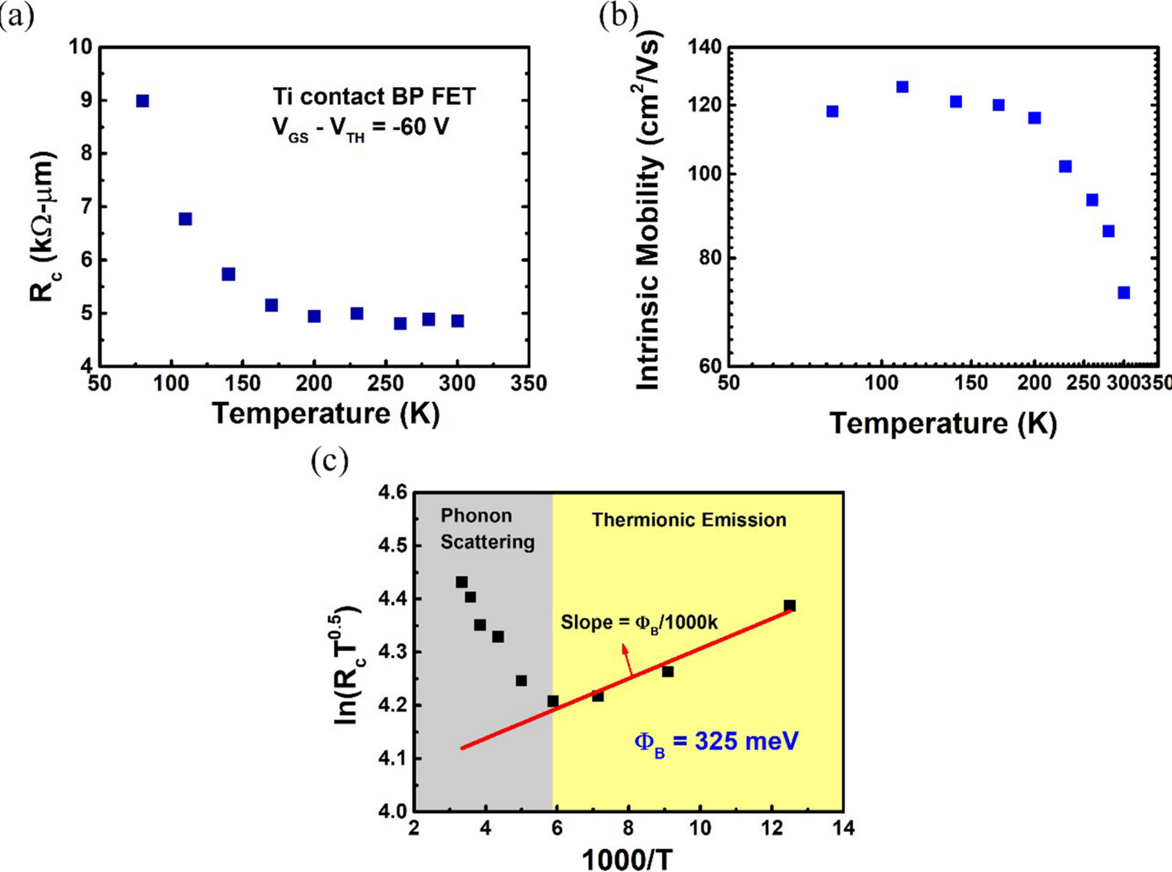

Figure 6. (a) Contact resistance (R_c) versus temperature. (b) Intrinsic mobility versus temperature, where phonon scattering is observed at $T > 200$ K. (c) The relationship between $\ln(R_cT^{0.5})$ and 1000/T, where a SBH of 325 meV is extracted from the slope.

layers) [19], this value accurately meets the theoretical E_{gap} of 0.41–0.42 eV. Consequently, we can plot the band alignment of BP and Ti. As shown in figure 4(b), a theoretical SBH of 0.228 eV is obtained. This value is consistent with the experimental SBH extraction results in [20], where the BP thickness is also 10 nm.

Compared the extracted SBH of 58.2 meV with the theoretical value analyzed above, there exists a significant discrepancy. To look into this deviation, consider the transfer curve with various temperatures shown in figure 3(a). A right-shift threshold voltage (V_{TH}) as temperature increases is observed, which results from thermionic emission current as discussed above. However, apart from thermionic emission, the interfacial traps between BP and SiO_2 interface and charge in dielectrics also result in a V_{TH} shift as temperature increases [21, 22], which can be observed in the hysteresis in the transfer curve. As shown in figure 5(a), the hysteresis of the same device is large at 300 K (~55 V),

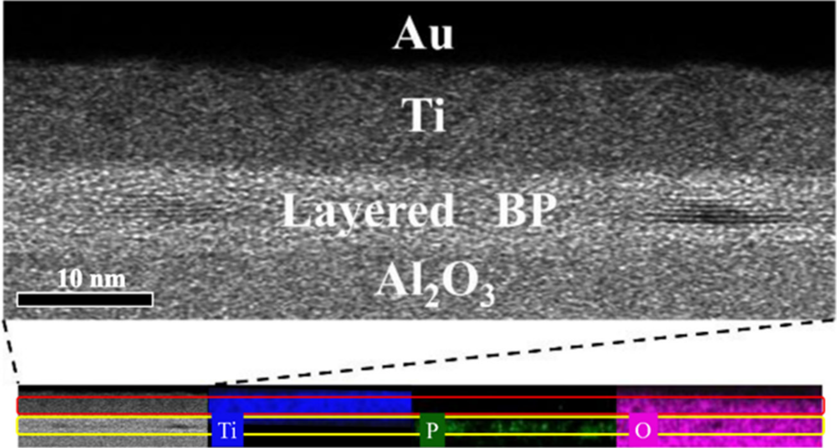

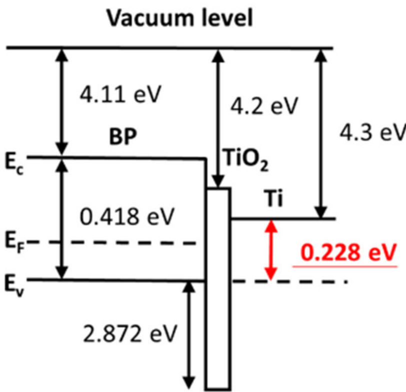

Figure 7. (a) TEM and EDX results of the Ti-BP junction contact. (b) Band alignment with TiO_2 added.

while it is almost negligible at 80 K. The almost-zero hysteresis can be attributed to the reduced interfacial trapping probability due to the low carrier concentration in the BP layer and longer trapping lifetime in the BP/SiO_2 interface at 80 K. Hysteresis defined as the V_{TH} difference of gate sweeping direction is also shown in figure 5(b) at various temperatures. As temperature increases beyond 170 K, hysteresis becomes significant and results in a left-shift of V_{TH} as gate voltage sweeps from negative to positive and a right-shift of V_{TH} as gate voltage sweeps from positive to negative. Consequently, in our transfer curve where V_{GS} sweeps from positive to negative, an extra right-shift of V_{TH}, which is equivalent to an increase of p-doping, causes higher I_{DS} at the sub-threshold regime, thus resulting in an underestimated SBH.

To avoid the effects of the hysteresis, we propose a modified method of SBH extraction utilizing the contact resistance formula of thermionic emission [23], $R_c = \frac{k}{qA^*T^{0.5}} e^{\frac{q\phi_B}{kT}}$, where the experimental R_c can be extracted by TLM at the same gate overdrive (V_{GS}–V_{TH}). There are two advantages in this method: (1) the effect of the extra V_{TH} shift can be eliminated at the same overdrive, and (2) the contact resistance avoids the deviation from the assumption that all of the V_{DS} drop at metal–semiconductor contact. The Schottky barrier height can be extracted by:

$$\ln\left(R_c T^{0.5}\right) = \text{const} + \frac{q\phi_B}{kT}. \quad (3)$$

Hence, we can extract the SBH by the slope of $\ln\left(R_c T^{0.5}\right)$ versus $1/T$. Note that the formula is only valid for the contact resistance of thermionic emission, which means at high gate overdrive (such as −90 V) the SBH will be underestimated due to the additional carrier injection of field emission. The extracted R_c at various temperatures at a gate overdrive of −60 V is plotted in figure 6(a). It is clear that R_c decreases as temperature increases. Before starting the extraction, effects of scattering should not be overlooked. As demonstrated in figure 6(b), the intrinsic mobility starts decreasing when temperature is higher than 170 K due to phonon scattering, resulting in a higher R_c [24]. Consequently, the extracted values may be deviated in high temperature regimes. As shown in figure 6(c), the relationship between $\ln\left(R_c T^{0.5}\right)$ versus $1000/T$ is plotted, where a turning point at 170 K is oberserved as expected. As a result, the relationship of R_c and temperature is dominated by two mechanisms: thermionic emission and phonon scattering. As temperature is lower than or equal to 170 K, thermionic emission dominates the temperature dependence of R_c, while phonon scattering becomes dominant at temperature higher than 170 K. Therefore, SBH is extracted in the range from 80 K to 170 K, where the value is 325 meV at gate overdrive of −60 V.

To examine the extracted value of 325 meV, Ti-BP contacts are also characterized by transmission electron microscopy (TEM) and energy-dispersive x-ray spectroscopy (EDX). Another few-layered BP is exfoliated and transferred to Al_2O_3/Si^{++} substrate, followed by 10/60 nm Ti/Au deposited by E-gun evaporator. As shown by the results in figure 7(a), the layered structures of BP are observed, although some of them disappear probably due to the damage caused by focused ion beam (FIB) process. Results of EDX in the same region are also shown in figure 7(a), where the region in the yellow frame is the BP layer. Since BP is vulnerable (easy to absorb) to H_2O and O_2 in the air, the oxidation process during the time interval between FIB and TEM will contribute to the oxygen signal in the EDX mapping. The region in the red frame is expected as the titanium deposited by E-gun evaporator. Also, the signal of O clearly exists in the Ti layer, indicating some part of Ti is oxidized to TiO_2 during deposition. TiO_2 may place an additional barrier for hole carriers as shown in figure 7(b) [25], which result in an increase of effective SBH of 325 meV. This value, however, might be varied form sample to sample due to different oxidation conditions and BP preparations. Consequently, from the comprehensive analysis discussed above, this modified extraction method reflects a more accurate SBH than the traditional method for the device due to the consideration of additional titanium oxide barrier.

Conclusion

In summary, we present the extraction of Schottky barrier height for a Ti contact BP FET by the activation energy method. Furthermore, the extracted Schottky barrier height is examined by theoretical estimation of Schottky–Mott rule. The activation energy method is found to underestimate the SBH due to the hysteresis at higher temperature. A modified extraction method of SBH by contact resistance is proposed, which could provide more accurate estimation of SBH. The extraction results demonstrate a SBH of 325 meV for our Ti contact BP transistor, which is in reasonable agreement with theoretical predictions and material characterization considerations.

Financial support

The financial support is provided by the Ministry of Science and Technology of Taiwan (R.O.C.) and Taiwan Semiconductor Manufacturing Company (TSMC) under MOST 106-2622-8-002-001, MOST 106-2218-E-005-001, MOST 106-2622-E-002-023-CC2 and MOST 105-2628-E-002-007-MY3.

Notes

The authors declare no competing financial interest.

ORCID iDs

Chao-Hsin Wu https://orcid.org/0000-0001-7849-773X

References

[1] Novoselov K S *et al* 2004 Electric field effect in atomically thin carbon films *Science* **306** 666–9
[2] Schwierz F 2010 Graphene transistors *Nat. Nanotechnol.* **5** 487–96
[3] Radisavljevic B, Radenovic A, Brivio J, Giacometti V and Kis A 2011 Single-layer MoS_2 transistors *Nat. Nanotechnol.* **6** 147–50
[4] Ganatra R and Zhang Q 2014 Few-layer MoS_2: a promising layered semiconductor *ACS Nano* **8** 4074–99
[5] Wu W *et al* 2013 High mobility and high on/off ratio field-effect transistors based on chemical vapor deposited single-crystal MoS_2 grains *Appl. Phys. Lett.* **102** 4
[6] Li L K *et al* 2014 Black phosphorus field-effect transistors *Nat. Nanotechnol.* **9** 372–7
[7] Nishii T, Maruyama Y, Inabe T and Shirotani I 1987 Synthesis and characterization of black phosphorus intercalation compounds *Synth. Met.* **18** 559–64
[8] Qiao J S, Kong X H, Hu Z X, Yang F and Ji W 2014 High-mobility transport anisotropy and linear dichroism in few-layer black phosphorus *Nat. Commun.* **5** 7
[9] Liu H, Du Y C, Deng Y X and Ye P D 2015 Semiconducting black phosphorus: synthesis, transport properties and electronic applications *Chem. Soc. Rev.* **44** 2732–43
[10] Long G *et al* 2016 Achieving ultrahigh carrier mobility in two-dimensional hole gas of black phosphorus *Nano Lett.* **16** 7768–73
[11] Du H W, Lin X, Xu Z M and Chu D W 2015 Recent developments in black phosphorus transistors *J. Mater. Chem.* C **3** 8760–75
[12] Penumatcha A V, Salazar R B and Appenzeller J 2015 Analysing black phosphorus transistors using an analytic Schottky barrier MOSFET model *Nat. Commun.* **6** 8948
[13] Deng Y, Conrad N J, Luo Z, Liu H, Xu X and Ye P D ed 2014 Towards high-performance two-dimensional black phosphorus optoelectronic devices: the role of metal contacts *2014 IEEE Int. Electron Devices Meeting (15–17 December 2014)* (https://doi.org/10.1109/IEDM.2014.7046987)
[14] Du Y C, Liu H, Deng Y X and Ye P D 2014 Device perspective for black phosphorus field-effect transistors: contact resistance, ambipolar behavior, and scaling *ACS Nano* **8** 10035–42
[15] Perello D J, Chae S H, Song S and Lee Y H 2015 High-performance n-type black phosphorus transistors with type control via thickness and contact-metal engineering *Nat. Commun.* **6** 7809
[16] Haratipour N and Koester S J 2016 Ambipolar black phosphorus MOSFETs with record n-channel transconductance *IEEE Electron Device Lett.* **37** 103–6
[17] Das S, Chen H-Y, Penumatcha A V and Appenzeller J 2013 High performance multilayer MoS_2 transistors with scandium contacts *Nano Lett.* **13** 100–5
[18] Allain A, Kang J H, Banerjee K and Kis A 2015 Electrical contacts to two-dimensional semiconductors *Nat. Mater.* **14** 1195–205
[19] Cai Y Q, Zhang G and Zhang Y W 2014 Layer-dependent band alignment and work function of few-layer phosphorene *Sci. Rep.* **4** 6
[20] Liu H *et al* 2014 Phosphorene: an unexplored 2D semiconductor with a high hole mobility *ACS Nano* **8** 4033–41
[21] Egginger M, Bauer S, Schwodiauer R, Neugebauer H and Sariciftci N S 2009 Current versus gate voltage

hysteresis in organic field effect transistors *Mon. Chem.* **140** 735–50

[22] Illarionov Y Y *et al* 2016 Long-term stability and reliability of black phosphorus field-effect transistors *ACS Nano* **10** 9543–9

[23] Chang C Y, Fang Y K and Sze S M 1971 Specific contact resistance of metal-semiconductor barriers *Solid-State Electron.* **14** 541

[24] English C D, Shine G, Dorgan V E, Saraswat K C and Pop E 2016 Improved contacts to MoS_2 transistors by ultra-high vacuum metal deposition *Nano Lett.* **16** 3824–30

[25] Jin L, Zhao H, Ma D, Vomiero A and Rosei F 2015 Dynamics of semiconducting nanocrystal uptake into mesoporous TiO_2 thick films by electrophoretic deposition *J. Mater. Chem.* A **3** 847–56